Food & Function

Linking the chemistry and physics of food with health and nutrition

Accepted Manuscript

This is an Accepted Manuscript, which has been through the Royal Society of Chemistry peer review process and has been accepted for publication.

Accepted Manuscripts are published online shortly after acceptance, before technical editing, formatting and proof reading. Using this free service, authors can make their results available to the community, in citable form, before we publish the edited article. We will replace this Accepted Manuscript with the edited and formatted Advance Article as soon as it is available.

You can find more information about Accepted Manuscripts in the Information for Authors.

Please note that technical editing may introduce minor changes to the text and/or graphics, which may alter content. The journal's standard Terms & Conditions and the Ethical guidelines still apply. In no event shall the Royal Society of Chemistry be held responsible for any errors or omissions in this Accepted Manuscript or any consequences arising from the use of any information it contains.

ROYAL SOCIETY OF CHEMISTRY

rsc.li/food-function

ARTICLE

UPLC-ESI-Q-TOF-MS^E -based metabolomics analysis of *Acer mono* Sap and evaluation for osteogenic activity in mouse osteoblast cells

Received 00th January 20xx,
Accepted 00th January 20xx

DOI: 10.1039/x0xx00000x

Karthi Natesan[a,#], Thimmarayan Srivalli[b,#], Harshavardhan Mohan[c], Arul Jayaprakash[b], and Vaikundamoorthy Ramalingam[d,e*]

Investigation of phytochemicals and bioactive molecules is tremendously vital for the applications of new plant resources in the chemistry, food and medicine. In the present study, the chemical profiling of sap of Acer mono (SAM), a Korean syrup known for anti-osteoporosis effect, was analysed using UPLC-ESI-Q-TOF-MS^E analysis. A total of 23 compounds were identified based on the mass and fragmentation characteristics and most of the compounds have significant biomedical applications. The *in vitro* antioxidant assessment of SAM exhibits excellent activity by scavenging the DPPH and ABTS free radicals and found to be 23.35 mg/mL and 29.33 mg/mL as IC_{50} concentration. As well, *in vitro* proliferation effect of the SAM was assessed against mouse MC3T3-E1 cells and the result showed that the SAM enhanced the proliferation of the cells and 12.5 and 25 mg/mL of SAM was selected for osteogenic differentiation. Morphological analysis clearly evidenced the SAM enhance the osteogenic activity in MC3T3-E1 cells by increased deposition of extracellular calcium and nodule formation. Moreover, the qRT-PCR analysis confirmed the increased expression of osteoblast marker gene expression including ALP, osteocalcin, osteopontin, collagen1α1, Runx2 and osterix in SAM treated MC3T3-E1 cells. Together, these results suggested that SAM possesses osteogenic effects and can be used for the bone regeneration and bone loss-associated diseases such as osteoporosis.

Keywords: Acer mono Sap; UPLC-ESI-Q-TOF-MS^E analysis; MC3T3-E1 cells; Osteogenesis; Molecular mechanism.

1. Introduction

Considering the global population size and its rapid growth rate, the osteoporosis likely to be a serious public health problem and most frequently screened bone disorder in humans [1]. Osteoporosis is characterised by decreased bone mineral density, deterioration and micro-architecture disruption, which is considered to be a major risk factor for bone fractures and disability [2] . In recent years, bone defects due to pathological infections, physiological disorders and resorption trauma are foremost challenge in orthopaedic surgery [3]. Epidemiological reports pinpoints the frequency of osteoporosis were observed in the major proportion of global population and its prevalence were found to be increased with age and depleted nutritious diet [4]. For past few decades, antiresorptive agents have been employed for the treatment of the serious bone disorder, epically estrogen and bisphosphonates are commonly prescribed against osteoporosis and are known for osteoclast inhibitory activity [5]. It is to be noted, prolonged use of the steroids and phosphonates are considered as major risk factor of breast cancer, nephrotic disorders like uterine bleeding and cardiovascular diseases [6]. Hence, the researchers focusing on the development of novel drugs for the treatment of osteoporosis without causing any side effects.

Currently, tremendous attentions focused towards plant-based foods and its derived food products that would possess versatile biological and pharmacological properties, which in turn helps in human health benefits [7]. Despite the recent investigation in last decades were based on herbs, plant products and mineral supplements to restore new bone formation following pathological conditions and to increase the bone mineral density to meet the necessity of the human body [8, 9]. Among, the Acer species have been traditionally used to treat various human diseases such as cancer, cardiovascular disorders, bone disorders, rheumatism, bruises, eye disease and detoxification [10]. To one side of Acer species as commercial uses, it is also used as traditional medicine in China, Japan, and Korea [11]. Particularly in Korea, the concentrated sap from maple trees especially Acer species are used as natural sweetener and are commonly called as sap of *Acer mono* (SAM) [12]. It is well documented that the SAM is the key source of minerals, monosaccharides and oligosaccharides, along with organic and amino acids, peptides, and proteins etc. [13]. As it consists of large amount of calcium and magnesium ion, SAM has been called as 'bone-benefit-water' [14].

Although SAM was traditionally used as folk medicine, as it possesses synergistic and versatile pharmacological effects, limited studies were done to define its functional aspects and modification.

[a]School of Allied Health Sciences, REVA University, Bengaluru, India
[b]Department of Chemistry, Research Institute of Physics and Chemistry, Jeonbuk National University, Jeonju 54896, Republic of Korea.
[c]PG and Research Department of Biochemistry, Scared Heart College (Autonomous), Tirupattur - 635601, Tamil Nadu, India. (Affiliated to Thiruvallur University, Serkkadu, Vellore – 632115, Tamil Nadu, India)
[d]Centre for Natural Products & Traditional Knowledge CSIR-Indian Institute of Chemical Technology, Hyderabad, India
[e]Academy of Scientific and Innovative Research (AcSIR), Ghaziabad – 201002, India
# Equal contribution.
*Corresponding Email: ramalingam@iict.res.in

To best of our knowledge, the use of SAM against osteogenic differentiation was not studied till now. Considering the beneficial effects of SAM, the present study was designed to discover the novel pharmacological effect of the SAM on induction of osteogenic differentiation in pre-osteogenic cells. In regard, various subsequent analyses were performed to investigate osteogenic differentiation and bone nodule formation on mouse pre-osteogenic cells.

2. Materials and methods

2.1. Chemicals and Reagents

The chemicals 1,1-diphenyl-2-picrylhydrazyl (DPPH), 2,2'-azino-bis(3-ethylbenzothiazoline-6-sulphonic acid) (ABTS) and ascorbic acid were obtained from Sigma Chemicals Co., USA. Potassium persulfate, dimethyl sulfoxide, methanol and all other chemicals were of analytical grade and purchased from common sources. Water was treated in a Milli-Q water purification system (TGI Pure Water Systems, USA).

2.2. Sample preparation

Maple syrup (grade C, 100 mL) was purchased from local market at Jeonju, Jeollabuk-Do, Republic of Korea. The syrup was maintained at -20°C and the subjected to liquid-liquid partitioning with water. The solvent was evaporated under rotary evaporator and aqueous extract yielded 2.8 gm, is further used for analysis.

2.3. Chemical profiling of SAM using UPLC-ESI-Q-TOF-MSE analysis

The chemical profiling of the SAM was executed on the Acquity H Class UPLC system (Waters, Milford, MA, USA) with an accustomed FTN auto sampler. An Acquity HSS T3 column (100 mm × 2.1 mm, 1.8 µm, Waters, Milford, MA, USA) was used for the chromatographic separation at 40 °C. The binary mobile phase was containing 0.1% formic acid in water (solvent A), 0.1% formic acid in acetonitrile (solvent B) and 0.1% formic acid in methanol (Solvent C) and Solvent C was pumped at 3% during the gradient elution. The flow rate was 0.4 mL/min. and the gradient elution was performed as follows: 0-1.0 min, 95% A; 1.0–3.0 min, 95%-77% A; 3.0–6.5 min, 77%-52% A; 10.0–14.0 min, 52%-37% A; 14.0–17.0 min, 37-12% A; 17.0–19.0 min, 12-2% A; 20.0–22.0 min equilibration performed, while 3 µL was used as injection volume.

To identify all the compounds from SAM, the total ion spectra was performed on Xevo G2-XS Q-TOF mass spectrophotometer (Waters, Machester, UK) with the mass range was 50-1500 *m/z*. The mass spectrometer was coupled with Electrospray ionization (ESI) and the analysis was performed in positive and negative modes with following conditions: the cone gas flow was 50 L/h and desolvation temperature was 350 °C, source temperature 120 °C, desolvation gas flow rate was 850 L/h and the Argon was used as CID gas for MS/MS analysis. Leucine – Enkephalin (1 ng/mL) was used as lock mass, generating a reference ion in positive/negative mode at m/z 556.2766/554.2620 and introduced by a lock spray at 5 µL/min for accurate mass acquisition. The MS^E program was employed for the simultaneous MS and MS/MS data collection and the obtained data information was presented as intact precursor ions and fragment ions. The data acquisition and processing were performed using UNIFI v.1.9 Scientific Information System (Waters, Manchester, UK) as described earlier [15].

2.4. Antioxidant activity

2.4.1. DPPH radical scavenging activity

DPPH assay was employed to assess the total free radical scavenging capacity of SAM according to the previously reported method with slight modifications [16]. In brief, the aliquots of completely dissolved SAM solution in various concentrations from 15.625 to 500 mg/mL was added to the freshly prepared 0.2 mM DPPH solution. The mixture was incubated in dark for 30 mins and the absorbance was recorded at 517 nm by using UV-VIS spectrophotometer (Shimadzu model 1800). The percentage of DPPH reduction is calculated taking into account the absorbance of blank solutions (DPPH solution in DMSO) and negative control (DMSO).

2.4.2. ABTS radical scavenging assay

ABTS cation decolorization assay was performed to evaluate the free radical scavenging activity of SAM according to the previously reported method [17]. Briefly, the ABTS free radicals are prepared by mixing 7 mM of ABTS with 2.45 mM of potassium persulfate in 1:1 ratio, and the solution was incubated in dark for 12 to 16 hr. Before use $ABTS^+$ solution was diluted with DMSO to obtain 0.700 absorbance at 734 nm. To aliquots of completely dissolved SAM solution in various concentrations from 15.625 to 500 mg/mL, the diluted $ABTS^+$ solution was added and incubated in dark for 30 minutes and the solvent was used as blank. All the measurements were carried out at least three times and the absorbance was measured at 734 nm. In scavenging of free radicals (DPPH and $ABTS^+$) was calculated as follows:

Scavenging activity (%) = (Control Abs.—Sample Abs.)/Control Abs × 100

Inhibition concentration 50% (IC_{50}) was determined by non-linear regression method using Graphpad prism software.

2.4.3. Ferric Reducing Antioxidant Potential (FRAP) Assay

Efficacy of SAM to scavenge free radicals was determined by FRAP assay with slight modifications [18]. Briefly, the freshly prepared FRAP solution was prepared by mixing the 300 mM acetate buffer, 10 mM TPTZ (2, 4, 6-tripyridyl-s-triazine) solution in 40 mM HCl and 20 mM $FeCl_3$ in the proportion of 10:1:1 ratio in volume. SAM at different concentration ranging from 15.625 to 500 were allowed to react with 3 mL of FRAP reagents at dark for 30 min at 37 °C. Blue coloured intensity of reduced Fe^{2+} -tripyridyltriazine by SAM were measured at 593 nm against a reagent blank (3.995 mL FRAP reagent+5 µL distilled water) after 30 min incubation at 37 °C. FRAP values were calculated by subtracting the difference between sample absorbance and blank absorbance. Reducing capacity in FRAP assay was calculated reference to the reaction signal given by an ascorbic acid solution. Final values of FRAP assay were expressed as nano-mole equivalent ascorbic acid/mg of SAM. All measurements were done in triplicate.

2.5. *In vitro* osteogenic activity

2.5.1. Cell culture

The MC3T3-E1 cells, a murine pre-osteoblast cell line, were purchased from KCLB, Seoul, Republic of Korea. The cells were cultured under standard condition in a 95% humidified atmosphere at 37°C and 5% CO_2 in basal α-MEM media (Hyclone, GE Healthcare) supplemented with heat-inactivated 10% fetal bovine serum (FBS) (v/v), 100 U/mL penicillin and 100 µg/mL streptomycin. The media were changed after a 24 h cell-attachment period and every 3 days. The cells were first cultured for 4 weeks under control conditions, allowing accumulation of extracellular matrix between cell layers and

used used in all subsequent experiments. Cells were plated in 60 mm tissue culture dishes and 96-well plates depend on respective assays.

2.5.2. Cell proliferation assay

Effect of SAM on MC3T3-E1 cells proliferation was determined by the MTT assay according to the previously reported method [19]. Briefly, about 1 × 10^4 cells were seeded in 96-well plates and incubated for 24 h to adhere. After, the cells were treated with 100 µL of various concentration of SAM (0.195 to 300 mg/mL) for 24 and 48 h. At the end of the treatment, the media with drug was replaced with 20 µL of freshly prepared MTT solution in PBS was added to each well and incubated for 4 h in a CO_2 incubator. The produced formazan crystals were dissolved with 100 µL of DMSO and the absorbance was recorded on a microplate reader at 570 nm. The effect of SAM on the cell proliferation and 50% of growth inhibition concentration were calculated.

2.5.3. Intracellular reactive oxygen species scavenging activity

To assess the antioxidant activity of SAM on MC3T3-E1 cells, the cells were treated with 0.1 mM H_2O_2 for 60 mins. After induce the oxidative stress, the cells were treated with various concentration of SAM (12.5 and 25 mg/mL respectively). After incubation for 24 h, the cells were washed with PBS and harvested. The cells were incubated with 25 µM of dichlorofluorescein diacetate (DCFDA) for 30 min at 37 °C in the dark. After washed with PBS, the fluorescence was captured using a FACSCalibur flow cytometer (BD Biosciences, San Jose, CA, USA). DCF fluorescence was measured at an excitation wavelength of 485 nm and emission wavelength of 540 nm [20].

2.5.4. Osteogenic differentiation

To investigate the SAM induced differentiation of MC3T3-E1 cells into matured osteoblast cells, the 5 days old culture of MC3T3-E1 cells was trypsinized and about 5 x10^4 cells were seeded in 6 well plates and grown in differentiation medium composed of complete α-MEM growth medium containing 10 mM β-glycerolphosphate and 0.25 mM ascorbic acid-2-phosphate in presence and absence of SAM (12.5 and 25 mg/mL) [21]. Whereas cells treated with 10 nM dexamethasone supplemented in DM served as positive control for osteogenic differentiation and the osteogenic effect of SAM alone was enumerated in presence or absence of DM.

2.5.5. Mineralization assay

Alizarin red S staining was performed to determine the hydroxyapatite deposition on cell matrix and bone nodule formation in SAM induced osteogenic differentiated cells. Cells were cultured in 6 well plates with or without differentiation medium and in presence or absence of SAM. After the treatment, the cells were observed for different time intervals (7, 14 and 21 days) for differentiation by staining the cells with ARS to assess the calcium deposition. In brief, after induce osteogenic differentiation the cells were gently washed twice with PBS and fixed with 10% neutral buffered formalin for 60 min at 4 °C. Further, the cells were stained with 5% ARS for 30 min at 37 °C and washed with deionized water to remove excess dye. The excess stain was removed with PBS and the stained matrix was photographed using a bright field inverted light microscope (Nikon, Japan) at 20x magnification [22]. The calcification of cellular matrix was further quantified by dissolve the staining solution with 10% (v/v) acetic acid digestion and addition of 500 µL mineral oil (Sigma–Aldrich) heated to 85°C for 10 min, followed with neutralization with 10% (v/v) ammonium hydroxide. The supernatant was collected after centrifugation at 20000 *g* and the absorbance was recorded at 405 nm in a transparent 96 well plate using microplate reader as previously described method with slight modifications [23].

2.5.6. Alkaline phosphatase activity staining

Effect of SAM on the alkaline phosphatase activity in MC3T3-E1 cells was determined by following the method described earlier (Ref). Briefly 5 x 10^5 cells were plated in 6-well plates and cells were subjected to osteogenic differentiation in presence or absence of SAM at two sub-GI50 concentration (12.5 and 25 mg/mL respectively) with or without differentiation medium. Followed by 1, 4, 7, 14, and 21 days of stimulated pre-osteogenic cell differentiation, cells were washed with PBS and fixed with 10% neutral buffered formalin for 60 sec. at 4 °C and monolayer cells were washed with wash buffer containing 0.05% Tween 20 in DPBS. Then, ALP staining was performed with a 1-Step™ NBT/BCIP (Cat No: 34042 Thermo Scientific) and ALP positive purple coloured stained cells images were documented using a bright field inverted light microscope (Nikon, Japan) at 20× magnification.

2.5.7. Real-time polymerase chain reaction (PCR)

MC3T3-E1 cells were plated at a density about 1.5 x 10^6 cells/ 100mm plate and incubated with or with our differentiation medium and in presence or absence of SAM at two different concentrations 12.5 and 25 mg/mL respectively. Total RNA was extracted from the control and treated cells on respective days after osteogenic stimulation (7, 14 and 21 days) using RNAiso Plus as per the manufacture's protocol (Takara, Cat. #9109) and quantified by using a UV spectrometer as described previously [24]. Total RNA was reverse-transcribed to produce first-strand cDNA using the TaKaRa reverse transcriptase (RT)-PCR Kit as per the manufactures protocol (TaKaRa Bio. Inc., Shiga, Japan). The expression of the bone related genes were determined by SYBR green-based real-time PCR analysis (Maxima SYBR Green/ROX qPCR Master Mix (2X) Thermo Scientific. The total volume of PCR reaction mixture is 10µL is containing 5 µL of SYBR green PCR master mix, 1 µL forward primer, 1 µL reverse primer and 1 µL 1 in 10 diluted cDNA and 2 µL of RNAase free DEPC water. The qPCR condition was performed as following initial denaturation at 95 °C for 10 min, the cycle start with denatured at 95 °C for 10 sec, annealing at 55~57 °C for 20 s, and extending at 72 °C for 30 sec for 30 cycles. Followed by melting curve to determine the specificity of the real-time PCR (55~95 °C, with 0.5 °C increment each cycle) [25]. Gene expression was normalized by the expression of house-keeping gene β-actin in the same sample. The data represented the average fold changes with standard error mean. All experiments were carried out in triplicate. The gene of interest and their respective forward and reverse primers are shown in Table S1.

2.6. Statistical analysis

All the experiments were carried out in triplicates and represented as the mean ± SEM respectively. The statistical difference between the treatment groups and its respective data were analysed with Prism 9 (GraphPad Software, La Jolla, CA). Significant different in osteogeinc treatment between different groups were analyzed by one-way analysis of variance (ANOVA) and Duncan's Multiple Range Test (DMRT) was conducted as post hoc test. Significance was established when * = $p < 0.05$, ** = $p < 0.01$,

3. Results and Discussion

The regenerative capacity of bone tissues in the large-area of bone damage is complicated and very hard to treat due to the limitations in the clinics [26]. Upon recognition of organic or inorganic compounds, the osteocytes act as mechanical sensors to repair the damage caused in the bone and improve the bone function [27]. During the repair mechanisms, the chemokines, cytokines and various growth factors are involved and behave as paracrine manner to enhance the bone repair [28]. There are several factors involved is involved in the osteogenic differentiation during bone repair and the chemical characteristic of the factors are key for promoting the environment conditions [29]. Owing to the aging, accidents, and unsafe sports, there is an urgent need for the therapeutic methods for bone repair and remodelling to enhance the osteogenesis. In the present study, the SAM was employed to stimulate the osteogenic differentiation in MC3T3-E1 cells and the chemical constituents responsible for the cell differentiation was determined using UPLC-Q-TOF-MS^E analysis.

Table 1 The list of compounds detected from the Acer mono Sap using UPLC-Q-TOF-MS^E analysis

No.	Proposed compound	Observed RT (min)	Expected mass (Da)	Observed mass (Da)	Observed m/z	Adducts	HRMS formula	Mass error (mDa)	Mass error (ppm)
1.	Caffeic acid	6.596207	180.0423	180.0416	181.0489	+H	$C_9H_8O_4$	-0.63908	-3.52988
2.	Carnosic acid	18.59006	332.1988	332.1982	371.1614	+K	$C_{20}H_{28}O_4$	-0.53645	-1.44533
3.	Coumaric acid	6.087874	164.0473	164.0464	165.0536	+H	$C_9H_8O_3$	-0.97716	-5.92021
4.	Daucosterol	19.10415	576.439	576.4352	577.4424	+H	$C_{35}H_{60}O_6$	-3.81978	-6.61495
5.	Ellagic acid	1.465355	302.0063	302.008	302.0074	-e	$C_{14}H_6O_8$	1.716443	5.68348
6.	Gallic acid	0.821963	170.0215	170.0222	188.056	+NH4	$C_7H_6O_5$	0.636163	3.382848
7.	Isorhamnetin	5.80831	316.0583	316.0606	316.0601	-e	$C_{16}H_{12}O_7$	2.339523	7.4022
8.	Kaempferide	8.40461	300.0634	300.0658	301.0731	+H	$C_{16}H_{12}O_6$	2.432725	8.080245
9.	Kaempferol	1.019622	286.0477	286.0449	287.0521	+H	$C_{15}H_{10}O_6$	-2.86754	-9.98952
10.	Lupeol	16.58461	426.3862	426.3894	427.3966	+H	$C_{30}H_{50}O$	3.201032	7.48966
11.	Methyl 4-hydroxycinnamate	5.55906	178.063	178.063	179.0703	+H	$C_{10}H_{10}O_3$	-0.01815	-0.10135
12.	Methyl ferulate	4.199616	208.0736	208.0736	209.0809	+H	$C_{11}H_{12}O_4$	0.059378	0.283996
13.	Methyl gallate	1.066208	184.0372	184.0379	202.0717	+NH4	$C_8H_8O_5$	0.73702	3.64733
14.	Myricetin	0.903974	318.0376	318.038	319.0453	+H	$C_{15}H_{10}O_8$	0.456741	1.431588
15.	Naringenin	5.300761	272.0685	272.0708	290.1047	+NH4	$C_{15}H_{12}O_5$	2.369221	8.166847
16.	Oleic acid	15.29898	282.2559	282.2534	283.2607	+H	$C_{18}H_{34}O_2$	-2.43035	-8.57983
17.	p-hydroxybenzoic acid	7.60009	122.0368	122.0359	123.0432	+H	$C_7H_6O_3$	-0.84735	-6.88655
18.	Pinoresinol	7.863144	358.1416	358.1411	359.1484	+H	$C_{20}H_{22}O_6$	-0.53472	-1.48886
19.	Quadranoside III	4.98972	666.3979	666.4048	705.3679	+K	$C_{36}H_{58}O_{11}$	6.855961	9.719789
20.	Quercetin 3-o-arabinoside	5.196343	434.0849	434.0852	435.0925	+H	$C_{20}H_{18}O_{11}$	0.329311	0.756877
21.	Rutin	4.939353	610.1534	610.1519	649.115	+K	$C_{27}H_{30}O_{16}$	-1.53261	-2.36107
22.	Sativanone	5.848335	300.0998	300.0971	301.1043	+H	$C_{17}H_{16}O_5$	-2.71588	-9.01965
23.	Scopoletin	6.057555	192.0423	192.0419	193.0492	+H	$C_{10}H_8O_4$	-0.38034	-1.97019
24.	Sinapic acid	5.235073	224.0685	224.0684	225.0757	+H	$C_{11}H_{12}O_5$	-0.05743	-0.25514
25.	Sitosterol	17.24761	414.3862	414.3845	453.3477	+K	$C_{29}H_{50}O$	-1.63174	-3.5993
26.	Ursolic acid	16.07631	456.3603	456.3634	495.3266	+K	$C_{30}H_{48}O_3$	3.079689	6.217531
27.	Ursolic acid acetate	16.58178	498.3709	498.3691	537.3322	+K	$C_{32}H_{50}O_4$	-1.81914	-3.3855

3.1. Chemical profiling of SAM

The ultra-performance liquid chromatography coupled with electrospray ionization quadrupole time-of- flight mass spectrometry (UPLC-ESI-Q-TOF-MS) has developed as a modern technique for identification and elucidation of metabolites in multifaceted extracts. In the present study, the high resolution total ion chromatogram of SAM was rapidly analysed using UPLC-Q-TOF-MSE analysed and the base intensity for SAM chromatogram in positive mode is showed in Fig. S1. The results depicted that the eighteen peaks were detected in positive ion mode and further TOF-MS and MS/MS analysis showed 27 compounds in the SAM (Table 1). As per our earlier study[15], the in house library was generated with the information acquired from Dictionary of Natural Products 30.2 (CRC Press, Taylor & Francis Group), PubMed, PubChem, ChemSpider etc. Further, the acquired information was imported into the UNIFI and compared with the raw UPLC-ESI-Q-TOF-MS^E data from low- and

high-energy collision scans. The compound identifications were made based on their MS and MS/MS spectral data such as exact mass and fragmentation pattern, retention times and finally compare the data with standard compounds (in-house library) and public database. For example, the compound Naringenin ($C_{15}H_{12}O_5$) $(M+H)^+$ was observed at *m/z* 272.257 (5.3 RT) in low collision energy MS^E mode (Fig. S2a) and the high collision energy MS^E mode of Naringenin was amply fragmented to 7 fragments ions (Fig. S2b) which were characterized based on their *m/z* value. The high-collision energy mode spectrum of Naringenin fragmented at *m/z* 167.18 ($C_9H_{11}O_3$), 195.16 ($C_9H_9O_3$), 152.05 ($C_8H_8O_3$), 137.15 ($C_8H_9O_2$), 135.04 ($C_8H_7O_2$), 119.04 (C_8H_7O), and 93.03 (C_6H_6O) (Fig. 1). As well, the Pinoresinol ($C_{20}H_{22}O_6$) (M+H)+ was observed at *m/z* 359.14 (7.86 RT) in low-collision energy (Fig. S3a) and fragmented into 10 fragments (Fig. S3b). The high-collision energy spectrum of Pinoresinol were detected at *m/z* 341.14 ($C_{20}H_{21}O_5$), 329.14 ($C_{19}H_{21}O_5$), 327.12 ($C_{19}H_{19}O_5$), 313.11 ($C_{18}H_{17}O_5$), 253.09 ($C_{16}H_{13}O_3$), 195.10 ($C_{11}H_{15}O_3$), 177.05 ($C_{10}H_9O_3$), 167.07 ($C_9H_{11}O_3$), 151.04 ($C_8H_7O_3$), and 137.06 ($C_8H_9O_2$) (Fig. 2). Based on these approach, about 27 compounds were identified in SAM and the compounds Gallic acid [30], methyl gallate [31], Kaempferol [32], Shikimic acid [33], Naringenin [34], Pinoresinol [35], Lupeol [36] and Ursolic acid [37] were known for their role in cell differentiation and tissue engineering applications (Fig. S4). The results recommended that the compounds in SAM could possible involve in the cell differentiation and we further determined the effect of SAM in the stimulation of osteogenic activity in MC3T3-E1 cells.

3.1. *In vitro* free radical scavenging activity of SAM

Freshly prepared solution of SAM with dimethyl sulfoxide was investigated for its primary antioxidant potential by DPPH assay at various concentrations from 500 to 0.061 mg/mL. Decolouration of purple coloured freshly prepared unstable DPPH solution to yellow coloured complex on reacting with bioactive compounds or extracts is confirmation of DPPH free radical scavenging property [38].

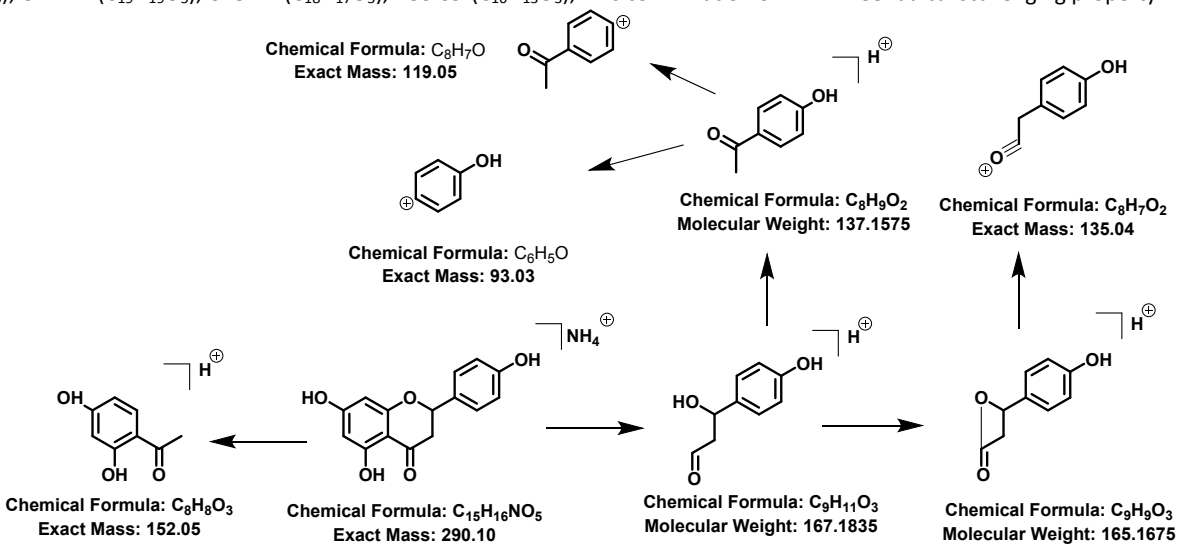

Fig. 1 Fragmentation of Naringenin isolated from the SAM

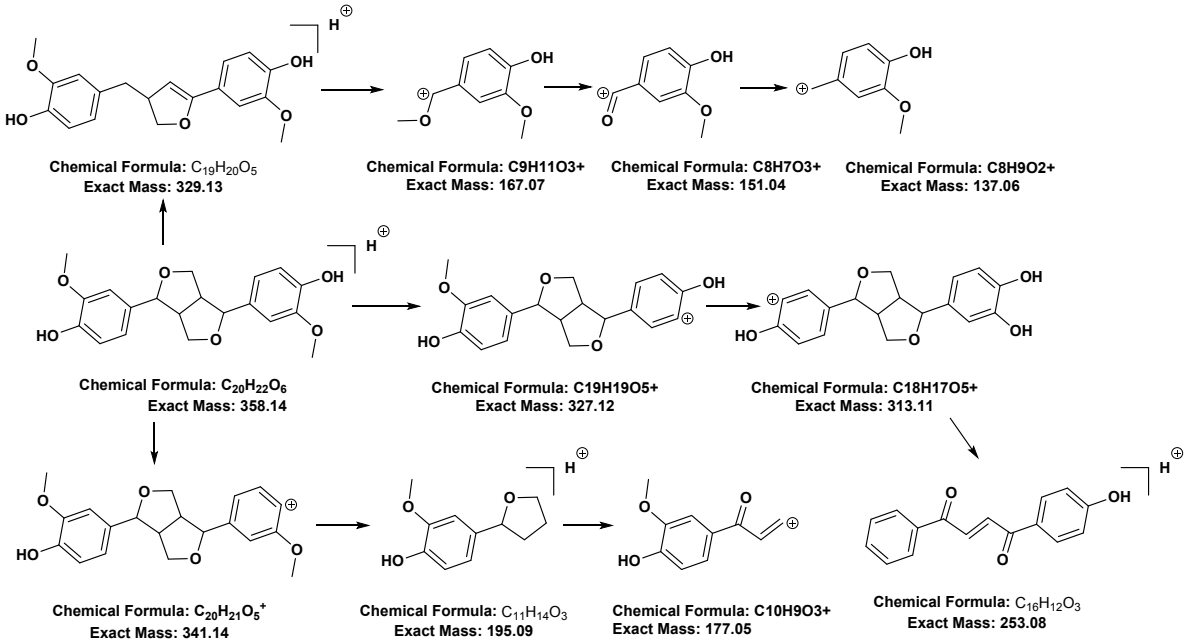

Fig. 2 Fragmentation of Pinorestinol isolated from the SAM

In the present study, the SAM is scavenging the DPPH in a concentration dependent manner and the yellow coloured complex was measured at 517 nm and about 23.35 mg/mL was determined as IC_{50} concentration using non-linear regression method (Fig. 3a). Further, the scavenging efficacy of SAM under aqueous medium was determined by ABTS scavenging assay. As showed in Fig. 3b, the SAM relative ability to scavenge the $ABTS^{+}$ generated in the aqueous by reacting potassium persulfate, which is a strong oxidizing agent with ABTS salt. The concentration dependent scavenging activity of SAM showed 29.33 mg/mL as IC_{50} concentration in which the SAM reduced the blue-green ABTS radical solution. Moreover, the effect of SAM on ferric reducing ability was evaluated by FRAP method and the results were measured to the equivalent ascorbic acid /mg. The reduction of Fe^{3+} to Fe^{2+} by affording the hydrogen atom is indicating the FRAP reduction capacity of the molecule [39]. In the present study, the SAM showed concentration dependent FRAP reduction activity and the the FRAP values for SAM was found to be range from 0.093 nM to 0.43 nM (Fig. 3c). Together, the SAM exhibited excellent *in vitro* scavenging activity and the bioactive compounds in the SAM responsible for the activity and possesses a strong antioxidant capacity.

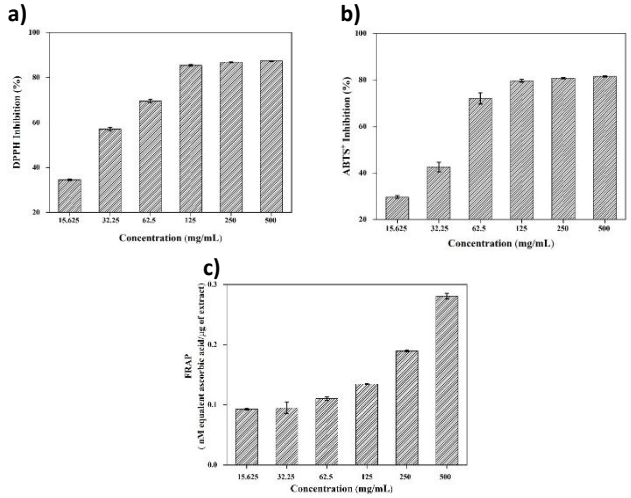

Fig. 3. *In vitro* antioxidant activity of SAM. *In-vitro* antioxidant potential of SAM was determined with different concentration using scavenging DPPH radical (a), scavenge ABTS radical (b) and ferric reducing capacity with FRAP assay (c). Values are expressed as mean ± SEM (n=3).

3.2. Effect of SAM on MC3T3-E1 cells proliferation

Osteoporosis is a result of bone broken which caused by the decreasing of estrogen certain medication, loss of bone mass, lack of sports exercises and smoking [40]. The induction of cell growth and differentiation of osteoblasts is evading the loss of bone mass and hinder the osteoporosis [41]. In the present study, the SAM was used to induce the growth and differentiation of MC3T3-E1 cells at two time intervals (24 & 48 h) to promote the osteogenesis. As showed in Fig. 4a, the SAM induce the cell proliferation in concentration dependent manner and increasing the concentration upto 300 mg/mL leads to inhibition of cellular growth. As well, the results showed that there is no toxicity up to 50 mg/mL and the 12.5 and 25 mg/mL of SAM was selected for further examination to stimulate the osteogenic differentiation in MC3T3-E1 cells.

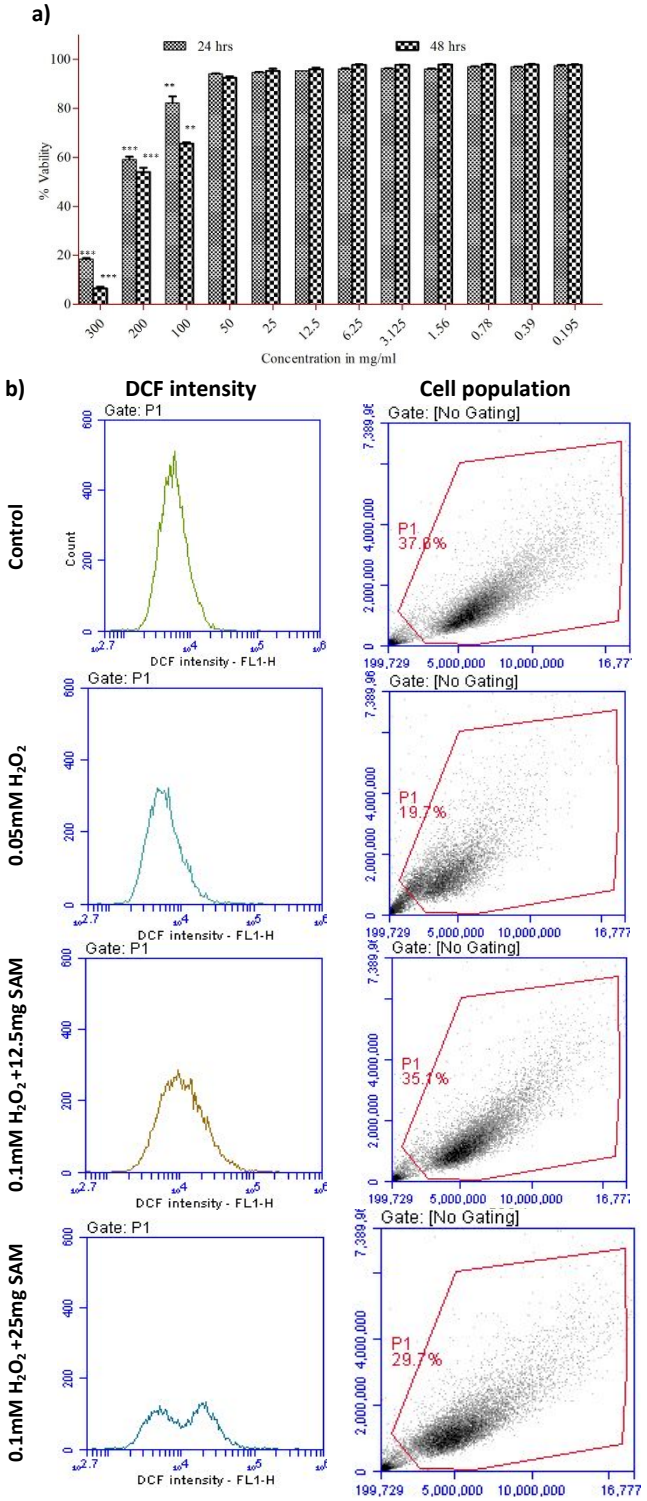

Fig. 4. Proliferation and antioxidant effect of SAM on MC3T3-E1 cells. SAM induced cell proliferation and cell viability on MCT3T3-E1 cells. Statistical data presented are the Mean ± SEM of results obtained from three independent experiments after 24 and 48 hr treatment. Antioxidant activity of SAM on MCT3T3T-E1 cells after treatment with 0.1 mM H_2O_2 was analysed by flow-cytometry for cytosolic ROS production. *** $P < 0.05$ compared with lower concentration and high concentration groups. Significant differences from lowest concentration were indicated by ***p<0.05 ***p<0.001* (considered as statistically significant).

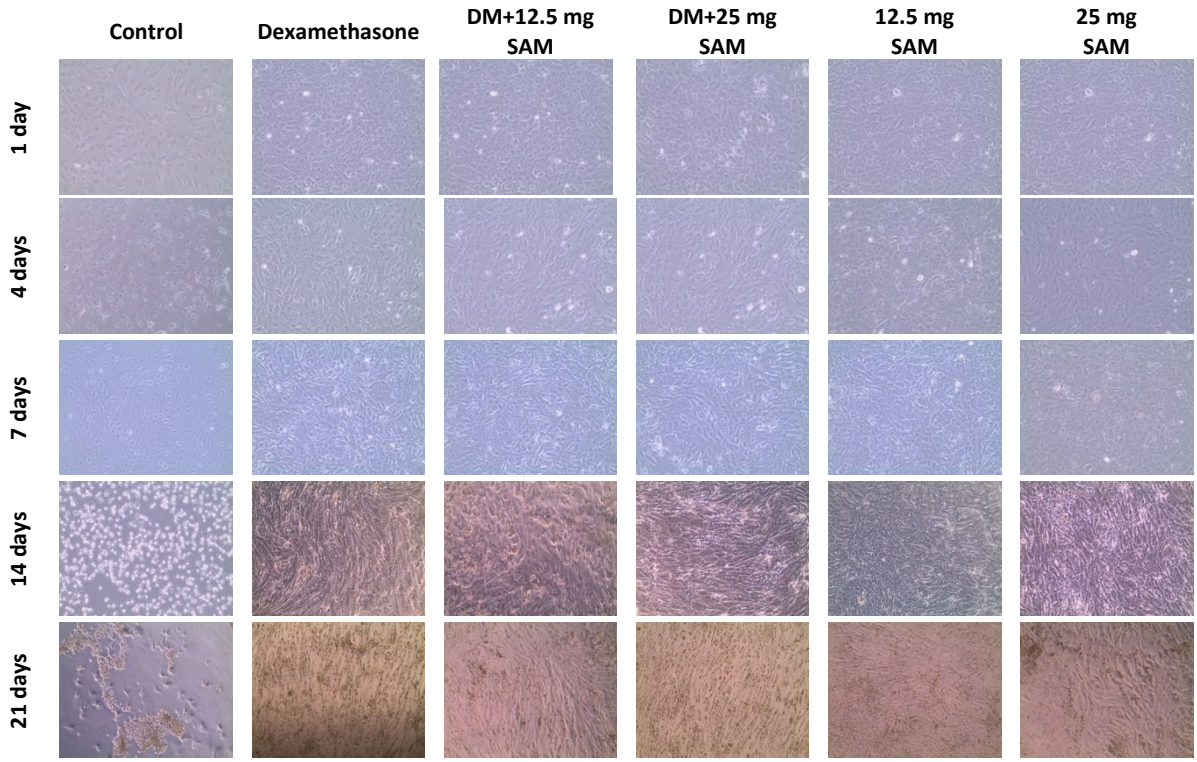

Fig. 5. SAM stimulated osteogenic morphological changes in MCT3T3-E1 cells. Morphological alterations during osteogenesis determined by inverted light microscopy on the day after induction at different time periods (i.e. day 1, 4, 7, 14 and 21 days). Images were photographed using a bright field inverted light microscope (Nikon, Japan) at 20× magnification and representative images are shown for each group.

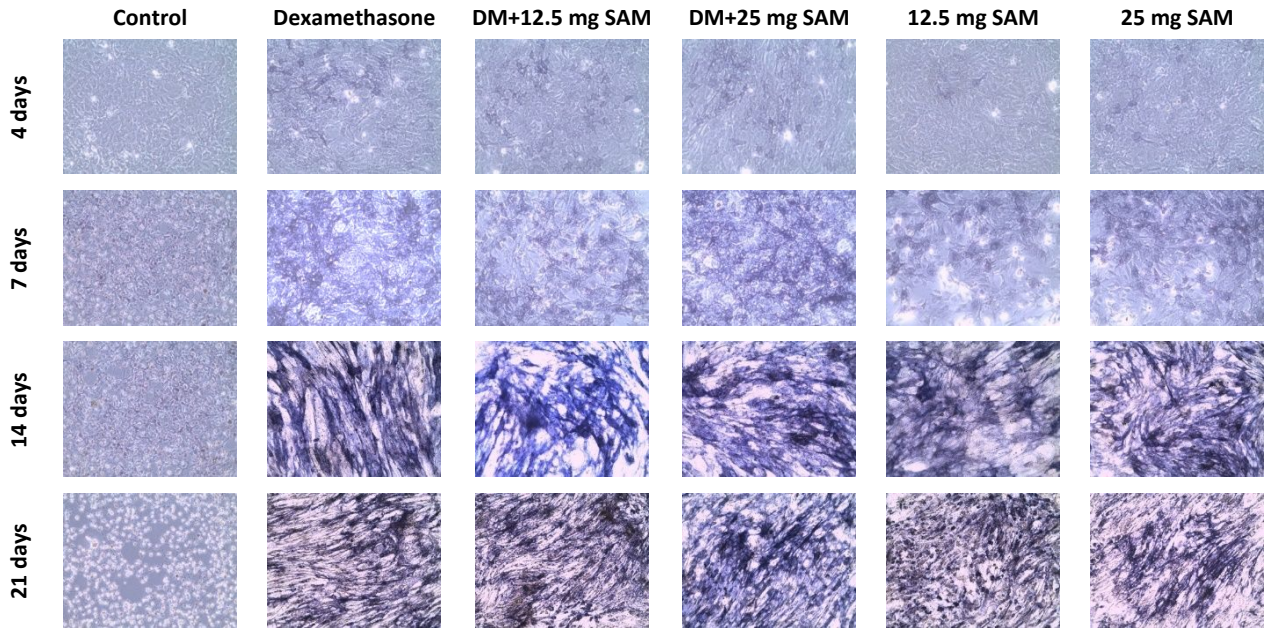

Fig. 6. NBT/BCIP staining for ALP activity on early osteoblast cells. Mouse pre-osteoblast MCT3T3-E1 cells were differentiated and stained for alkaline phosphatase activity after 4, 7, 14 and 21 days after induction. Images were photographed using a bright field inverted light microscope (Nikon, Japan) at 20× magnification and representative images are shown for each group.

3.3. Antioxidant potential of SAM against intracellular ROS

Antioxidants are play a key role by contributing directly or counteracting the activation or inducing the differentiation of osteoblasts, mineralization process and the reduction of osteoclast activity [42]. The redox homeostasis in the cells are also favouring for differentiation by regulating the key phosphatases and kinases [43]. In

the present study, the antioxidant effect of SAM was assessed against the H_2O_2 stimulated MC3T3-E1 cells. As showed in Fig. 4b, the SAM decreasing the oxidative stress induced by H_2O_2 in MC3T3-E1 cells in concentration dependent manner is confirmed by fluorescent intensity using Flow cytometry analysis. As well, the quantified amount of fluorescence after treatment with different concentration of SAM was directly proportional to the intracellular ROS generated in the pre-osteogenic cells. The results are indicating the SAM significantly neutralize the free radicals and intracellular ROS generation in H_2O_2 stimulated MC3T3-E1 cells.

3.4. Morphologic alteration during SAM induced osteogenesis on MC3T3-E1 cells

Cell architectural alterations during SAM induced osteogenic differentiation in murine mouse pre-osteogenic cells were observed for a period of 21 days. As shown in Fig. 5, the treatment with SAM in presence or absence of differentiation medium on MC3T3-E1 cells were compared with positive drug control dexamethasone treated cells. The results clearly evidenced that the osteogenic differentiation was induced in the cells with SAM in presence/absence of differentiation medium and significantly stimulated the osteogenesis at all tested concentration. Further on comparing, SAM at 15 and 25 mg/mL concentration with DM had more significantly osteogenic differentiation than in cells treated without DM. Moreover, 25 mg SAM in absence of DM also had shown a significant osteogenic induction on MC3T3-E1 cells is evidence by the loss of typical polyhedral and round shaped morphology to matured fibroblasts displaying a fibroblast-like morphology with unordered cellular arrangement. Cells during the stage of maturation from 14 days after stimulation to 21 days, minerals deposits were noted as black dots over the cell monolayers confirm the mature osteoblast cells.

3.5. SAM induced alkaline phosphatase activity

The early stages of osteogenic differentiation were evident by increased ALP activity. MC3T3-E1cell monolayer treated with or without differentiation medium in presence and absence of SAM were stained using NBT/BCIP staining kit at different time interval. ALP is an early-stage marker of osteogenesis which promotes the mineralization of the osteoblast cells during the osteogenic process [44]. As showed in Fig. 6, the SAM significantly increased the ALP activity in dose dependent manner is also evidently confirmed by the osteogenic differentiation in the presence and absence of differentiation medium. Initially, the cells showed the increased ALP activity which showed by the purple colored chromogen end product is the resultant of the ALP catalyzation by NBT reaction. As well, the cells treated with SAM in absence of DM also showed a significant ALP activity, however the morphology and the ALP activity were found to be more prominent than the cells treated with SAM in presence of DM. Conviction of this ALP staining assay discernibly proved that SAM significantly induce osteogenic differentiation in mouse per-osteogenic cells.

3.6. SAM induced calcified nodule formation in osteoblast cells.

The ALP activity is enhanced during osteogenic differentiation by observing the dark purple granules which is the resultant of red calcium deposition [45]. In the present study, the formation of calcium nodules during late and matured osteoblast differentiation of MC3T3-E1 cells were quantified by Alizarin Red S (ARS) staining method. As showed in Fig. 7, the treatment of SAM increased calcium deposited cell matrix on DM induced MC3T3-E1 cells was observed as comparing with control cells and also significant calcium deposition was observed in the cells treated with SAM. Initially at 7 days ARS staining showed no difference between basal and osteogenic condition and increase the treatment period to 21 days showed the matured osteoblast cells with calcification and nodule formation as compared with dexamethasone treated cells. Further, the spectrometric quantification showed the amount of calcium deposited over the cell matrix were significantly higher in the cells treated with SAM in presence/absence of DM were observed. Previously reported that the elevated levels of calcium and phosphate in the cells leads to the induced calcification and subsequently promote the cell differentiation [46]. Interestingly, the significant amount of calcium deposited on cells treated in absence of DM stimulated cells than the absence of DM stimulation. Together, the results indicated that the formation of calcium nodules were simulated on treatment with SAM in MC3T3-E1 cells.

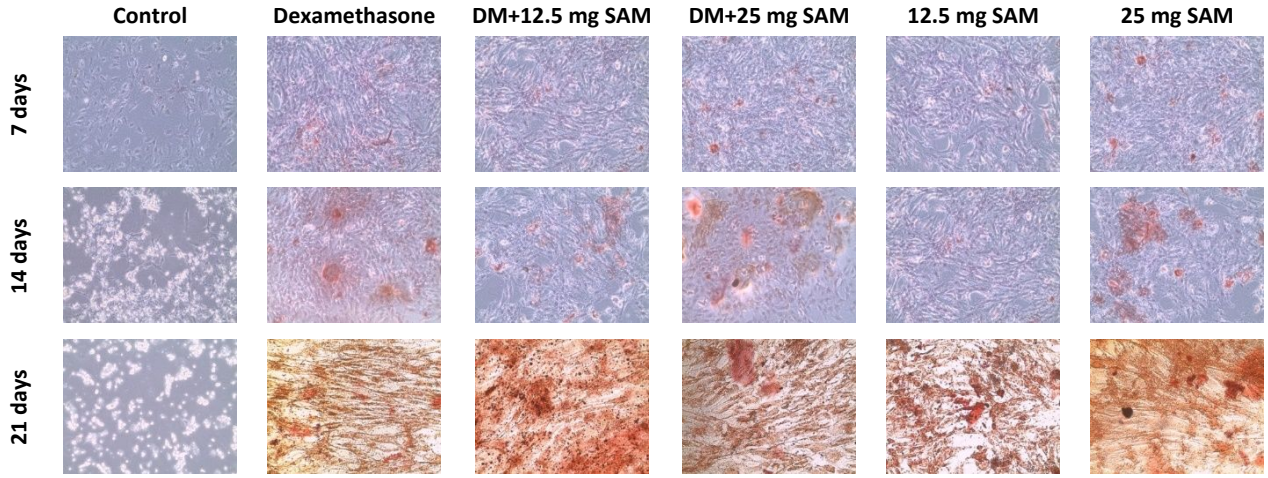

Fig. 7. Alizarin Red S staining for SAM induced calcification on MCT3T3-E1 cells. a) Cells were grown and treated with/without 12.5 and 25 mg/mL of SAM and subjected to a rapid staining protocol for osteogenic differentiation at 7, 14 and 21 days after stimulation for matrix mineralization by Alizarin Red S. The images were recorded with inverted light microscope at 20 x magnification.

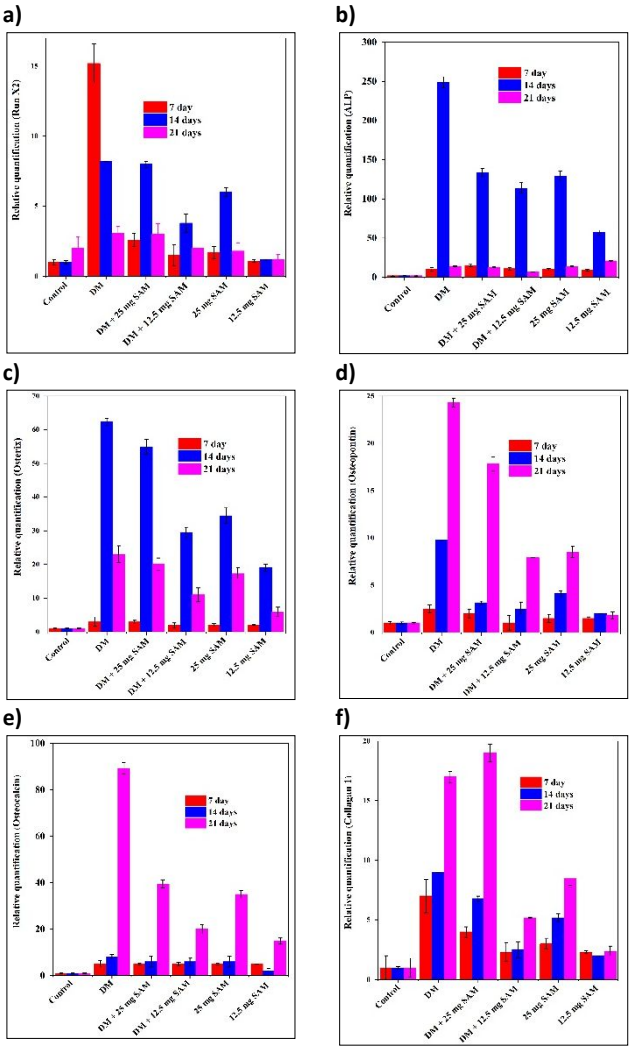

Fig. 8. Effects of SAM on the mRNA expression of bone related gene. Cells were cultured with/without 12.5 and 25 mg/mL concentration of SAM for 7, 14 and 21 days after induction. Total RNA was isolated and the level of the target gene expression was determined by real-time PCR. The values obtained for the target gene expression were normalized to β-actin and relatively quantified to the expression in non-stimulated control cells. The data presented are representative of two independent experiments.

3.7. Gene expression profile of SAM stimulated osteogenic differentiated cells.

The osteoblast differentiation is regulated by different transcription factors, in which the Runt-related transcription factor 2 (Runx2) is playing key role in the osteogenesis and the knockout or mutations in Runx2 is leads to the bone dysplasia or bone related disorders [47]. In the present study, the treatment of MC3T3-E1 cells with SAM upregulates the expression of Runx2 and the similar expression level was observed in the cells treated with dexamethasone (Fig. 8a). Runx2 regulates the proliferation of osteoblast progenitors and their differentiation into osteoblasts [48] and Runx2 is essential for the regulation of multiple osteogenic genes including collagen I, osteopontin, alkaline phosphatase (ALP), bone and osteocalcin [49]. Among, the ALP is an early marker gene for the osteogenic differentiation and highly expressed in the cells during growth plate calcification to develop the hard tissue [50]. At early stage of SAM induced osteogenesis the proliferation of MC3T3-E1 cells were downregulated, whereas the ALP gene was significantly upregulated at 7 and 14 days which were downregulated in matured osteoblast at 21 days (Fig. 8b) is clearly indicating the SAM induce the osteogenic differentiation by regulating the ALP in early stage of differentiation. It is well known that ALP expression was induced by over expression of osterix (Osx) gene, as well, the SAM treated cells showed increased expression of Osx gene as compared with control cells (Fig. 8c). Osx is an osteoblast-specific transcription factor predominantly involves in the activation of genes responsible for differentiation of preosteoblasts into mature osteoblasts and osteocytes [51].

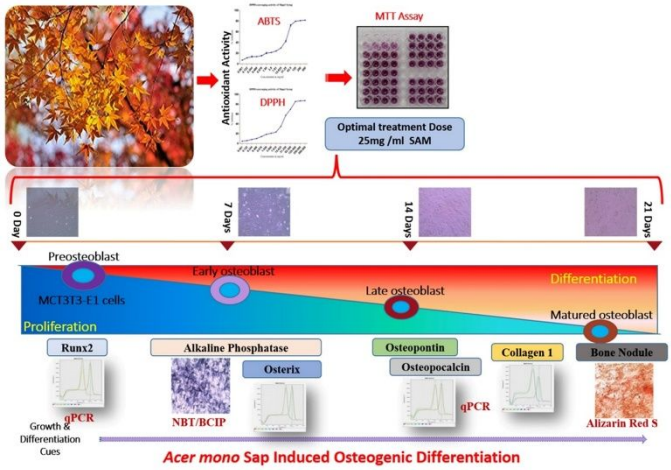

Fig. 9. Schematic representation of SAM stimulating the osteogenic differentiation on MCT3T3-E1 cells.

Apart from the early marker gene ALP, the Runx2 also regulates the type I collagen (Col-I), and the late marker genes are osteopontin (OPN) and osteocalcin (OCN) [52]. In the present study, the SAM treatment also stimulate the up-regulation of OPN than the control and dexamethasone treated MC3T3-E1 cells (Fig. 8d). Finally, the genes OCN and Coll-I, which are responsible for the deposition and maturation of bone extracellular matrix expression were determined and the results showed that the OCN and Coll-I upregulated at 21 day of SAM stimulation in MC3T3-E1 cells (Fig. 8e & 8f). It has been demonstrated that the Type I Col is the abundantly found in the extracellular matrix and main molecule of interest for proliferation, survival, adhesion and osteogenesis [53]. Together, the gene expression profile on SMA stimulated osteogenesis evidently pinpoint the osteogenic differentiation in mouse pre-osteogenic MC3T3-E1 cells. As well, the UPLC-ESI-Q-TOF-MS^E results also uncovered the presence of active constituents, hence the SAM can be used to test against animal model.

4. Conclusion

In conclusion, the present study indicates the SAM efficiently stimulate the osteoblast differentiation in *in vitro* cell model. Initially, the chemical profiling of SAM using UPLC-Q-TOF-MS^E analysis showed the potential nutraceuticals and bioactive compounds are involving in the developmental stages including proliferation, bone

matrix formation/maturation, and mineralization. Further, the SAM induce the proliferation and differentiate the pre-osteoblast to matured osteoblast by inhibit the ROS generation. The nutraceutical composition of SAM actively involved in the calcification of mouse cells and induces the nodule formation in mature osteoblast. As well, the SAM regulates the key osteogenic marker genes such as Runx2, ALP, Osx, Col-I. OPN and OCN which are known for proliferation, survival, adhesion and osteogenesis (Fig. 9). Together, the results indicated that the SAM can be used as a food ingredient and used for the bone regeneration and treatment of bone related disorders

Acknowledgement

Author acknowledge the authorities of the Jeonbuk National University for providing the facilities to complete the study. VR acknowledge the Director, CSIR-Indian Institute of Chemical Technology, Hyderabad for his keen interest on the work. The IICT communication number is IICT/Pubs./2022/204.

References

1. L. C. Hofbauer, B. Busse, R. Eastell, S. Ferrari, M. Frost, R. Müller, A. M. Burden, F. Rivadeneira, N. Napoli and M. Rauner, Bone fragility in diabetes: novel concepts and clinical implications, *The Lancet Diabetes & Endocrinology*, 2022, **10**, 207-220.
2. T. Sozen, L. Ozisik and N. Calik Basaran, An overview and management of osteoporosis, *European Journal of Rheumatology*, 2017, **4**, 46-56.
3. J. Baharara, T. Ramezani, M. Mousavi and M. J. J. o. H. P. Asadi-Samani, Synergistic effect of pulsed electromagnetic fields and saffron extract on osteogenic differentiation of bone marrow mesenchymal stem cells, 2017, **6**.
4. C. Cooper, E. M. Dennison, N. R. Fuggle, E. M. Curtis, N. C. Harvey and M. A. Clynes, The epidemiology of osteoporosis, *British Medical Bulletin*, 2020, DOI: 10.1093/bmb/ldaa005, 105–117.
5. C. Zhang and C. Song, Combination Therapy of PTH and Antiresorptive Drugs on Osteoporosis: A Review of Treatment Alternatives, *Frontiers in Pharmacology*, 2021, **11**, 607017.
6. J. H. Hwang, P. H. Cha, G. Han, T. T. Bach, S. Min do and K. Y. Choi, Euodia sutchuenensis Dode extract stimulates osteoblast differentiation via Wnt/beta-catenin pathway activation, *Experimental & molecular medicine*, 2015, **47**, e152.
7. M. Nikbakht Nasrabadi, A. Sedaghat Doost and R. Mezzenga, Modification approaches of plant-based proteins to improve their techno-functionality and use in food products, *Food Hydrocolloids*, 2021, **118**.
8. P. Singh, A. Gupta, I. Qayoom, S. Singh and A. Kumar, Orthobiologics with phytobioactive cues: A paradigm in bone regeneration, *Biomedicine & Pharmacotherapy*, 2020, **130**, 110754.
9. R. Abdul Rahim, P. A. Jayusman, V. Lim, N. H. Ahmad, Z. A. Abdul Hamid, S. Mohamed, N. Muhammad, F. Ahmad, N. Mokhtar, N. Mohamed, A. N. Shuid and I. Naina Mohamed, Phytochemical Analysis, Antioxidant and Bone Anabolic Effects of Blainvillea acmella (L.) Philipson, *Frontiers in Pharmacology*, 2022, **12**, 796509.
10. M.-V. Hovanet, N. Dociu, M. Dinu, R. Ancuceanu, E. Morosan and E. J. R. C. Oprea, A comparative physico-chemical analysis of Acer platanoides and Acer pseudoplatanus seed oils, 2015, **66**, 987-991.
11. W. Bi, Y. Gao, J. Shen, C. He, H. Liu, Y. Peng, C. Zhang and P. Xiao, Traditional uses, phytochemistry, and pharmacology of the genus Acer (maple): A review, *Journal of Ethnopharmacology*, 2016, **189**, 31-60.
12. G. Q. N'guyen, N. Martin, M. Jain, L. Lagacé, C. R. Landry and M. Filteau, A systems biology approach to explore the impact of maple tree dormancy release on sap variation and maple syrup quality, *Scientific Reports*, 2018, **8**, 14658.
13. A. Saraiva, C. Carrascosa, D. Raheem, F. Ramos and A. Raposo, Natural Sweeteners: The Relevance of Food Naturalness for Consumers, Food Security Aspects, Sustainability and Health Impacts, *International Journal of Environmental Research and Public Health*, 2020, **17**.
14. E. Pereira, L. Barros and I. C. Ferreira, Relevance of the Mention of Antioxidant Properties in Yogurt Labels: In Vitro Evaluation and Chromatographic Analysis, *Antioxidants (Basel, Switzerland)*, 2013, **2**, 62-76.
15. V. Ramalingam, N. Narendra Kumar, M. Harshavardhan, H. M. Sampath Kumar, A. K. Tiwari, K. Suresh Babu and M. K. R. Mudiam, Chemical profiling of marine seaweed Halimeda gracilis using UPLC-ESI-Q-TOF-MSE and evaluation of anticancer activity targeting PI3K/AKT and intrinsic apoptosis signaling pathway, *Food Research International*, 2022, **157**.
16. V. Ramalingam and R. Rajaram, 2-Ethoxycarbonyl-2-β-hydroxy-a-nor-cholest-5-ene-4one: Extraction, structural characterization, antimicrobial, antioxidant, anticancer and acute toxicity studies, *Steroids*, 2018, **140**, 11-23.
17. C. Fu, H. Bai, Q. Hu, T. Gao and Y. J. R. A. Bai, Enhanced proliferation and osteogenic differentiation of MC3T3-E1 pre-osteoblasts on graphene oxide-impregnated PLGA–gelatin nanocomposite fibrous membranes, 2017, **7**, 8886-8897.
18. I. F. Benzie and J. J. Strain, The ferric reducing ability of plasma (FRAP) as a measure of "antioxidant power": the FRAP assay, *Analytical biochemistry*, 1996, **239**, 70-76.
19. V. Ramalingam and I. Hwang, Zero valent zinc regulates adipocyte differentiation through calpain family protein and peroxisome proliferator-activated receptor gamma signaling in mouse 3T3-L1 cells, *Process Biochemistry*, 2021, **101**, 285-293.
20. V. Ramalingam, S. Raja and M. Harshavardhan, *In situ* one-step synthesis of polymer-functionalized palladium nanoparticles: an efficient anticancer agent against breast cancer, *Dalton Transactions*, 2020, **49**, 3510-3518.
21. P. Naruphontjirakul, A. E. Porter and J. R. Jones, In vitro osteogenesis by intracellular uptake of strontium containing bioactive glass nanoparticles, *Acta biomaterialia*, 2018, **66**, 67-80.
22. X. Wen, X. Li, Y. Tang, J. Tang, S. Zhou, Y. Xie, J. Guo, J. Yang, X. Du, N. Su and L. Chen, Chondrocyte FGFR3 Regulates Bone Mass by Inhibiting Osteogenesis, *Journal of Biological Chemistry*, 2016, **291**, 24912-24921.
23. A. Spina, R. Montella, D. Liccardo, A. De Rosa, L. Laino, T. A. Mitsiadis and M. La Noce, NZ-GMP Approved Serum Improve hDPSC Osteogenic Commitment and Increase Angiogenic Factor Expression, *Frontiers in Physiology*, 2016, **7**, 354.
24. V. Ramalingam and I. Hwang, Deciphering the significant role of various gene expression in modulating the toughness of bovine muscle, *Biocatalysis and Agricultural Biotechnology*, 2021, **31**.
25. V. Ramalingam and I. Hwang, Identification of Meat Quality Determining Marker Genes in Fibroblasts of Bovine Muscle Using Transcriptomic Profiling, *Journal of Agricultural and Food Chemistry*, 2021, **69**, 3776-3786.

26. P. Zhou, J.-M. Shi, J.-E. Song, Y. Han, H.-J. Li, Y.-M. Song, F. Feng, J.-L. Wang, R. Zhang and F. Lan, Establishing a deeper understanding of the osteogenic differentiation of monolayer cultured human pluripotent stem cells using novel and detailed analyses, *Stem Cell Research & Therapy*, 2021, **12**, 41.
27. M. Valenti, L. Dalle Carbonare and M. Mottes, Osteogenic Differentiation in Healthy and Pathological Conditions, *International Journal of Molecular Sciences*, 2016, **18**, 41.
28. E. Mazzoni, C. Mazziotta, M. R. Iaquinta, C. Lanzillotti, F. Fortini, A. D'Agostino, L. Trevisiol, R. Nocini, G. Barbanti-Brodano, A. Mescola, A. Alessandrini, M. Tognon and F. Martini, Enhanced Osteogenic Differentiation of Human Bone Marrow-Derived Mesenchymal Stem Cells by a Hybrid Hydroxylapatite/Collagen Scaffold, *Frontiers in Cell and Developmental Biology*, 2021, **8**, 610570.
29. G. Mestres, S.-S. D. Carter, N. P. Hailer and A. Diez-Escudero, A practical guide for evaluating the osteoimmunomodulatory properties of biomaterials, *Acta Biomaterialia*, 2021, **130**, 115-137.
30. Y. Oh, C.-B. Ahn, M. P. C. K. Marasinghe and J.-Y. Je, Insertion of gallic acid onto chitosan promotes the differentiation of osteoblasts from murine bone marrow-derived mesenchymal stem cells, *International Journal of Biological Macromolecules*, 2021, **183**, 1410-1418.
31. J. Baek, J.-Y. Kim, C. Lee, K.-H. Yoon and M. Lee, Methyl Gallate Inhibits Osteoclast Formation and Function by Suppressing Akt and Btk-PLCγ2-Ca2+ Signaling and Prevents Lipopolysaccharide-Induced Bone Loss, *International Journal of Molecular Sciences*, 2017, **18**.
32. F. Nie, W. Zhang, Q. Cui, Y. Fu, H. Li and J. Zhang, Kaempferol promotes proliferation and osteogenic differentiation of periodontal ligament stem cells via Wnt/β-catenin signaling pathway, *Life Sciences*, 2020, **258**.
33. Y.-W. Kwon, S.-H. Lee, A.-R. Kim, B. J. Kim, W.-S. Park, J. Hur, H. Jang, H.-M. Yang, H.-J. Cho and H.-S. Kim, Plant callus-derived shikimic acid regenerates human skin through converting human dermal fibroblasts into multipotent skin-derived precursor cells, *Stem Cell Research & Therapy*, 2021, **12**, 346.
34. M. Pellegrini, P. Bulzomi, P. Galluzzo, M. Lecis, S. Leone, V. Pallottini and M. Marino, Naringenin modulates skeletal muscle differentiation via estrogen receptor α and β signal pathway regulation, *Genes & Nutrition*, 2014, **9**, 425.
35. M. V. Sepporta, T. Mazza, G. Morozzi and R. Fabiani, Pinoresinol Inhibits Proliferation and Induces Differentiation on Human HL60 Leukemia Cells, *Nutrition and Cancer*, 2013, **65**, 1208-1218.
36. F. Pereira Beserra, M. Xue, G. Maia, A. Leite Rozza, C. Helena Pellizzon and C. Jackson, Lupeol, a Pentacyclic Triterpene, Promotes Migration, Wound Closure, and Contractile Effect In Vitro: Possible Involvement of PI3K/Akt and p38/ERK/MAPK Pathways, *Molecules*, 2018, **23**.
37. M. Kim, B. Sung, Y. J. Kang, D. H. Kim, Y. Lee, S. Y. Hwang, J.-H. Yoon, M.-A. Yoo, C. M. Kim, H. Y. Chung and N. D. Kim, The combination of ursolic acid and leucine potentiates the differentiation of C2C12 murine myoblasts through the mTOR signaling pathway, *International Journal of Molecular Medicine*, 2015, **35**, 755-762.
38. V. Ramalingam and R. Rajaram, Antioxidant activity of 1-hydroxy-1-norresistomycin derived from Streptomyces variabilis KP149559 and evaluation of its toxicity against zebra fish Danio rerio, *RSC Advances*, 2016, **6**, 16615-16623.
39. V. Ramalingam and R. Rajaram, Enhanced antimicrobial, antioxidant and anticancer activity of Rhizophora apiculata: An experimental report, *3 Biotech*, 2018, **8**, 200.
40. H. Chen, Z. Xu, F. Fan, P. Shi, M. Tu, Z. Wang and M. Du, Identification and mechanism evaluation of a novel osteogenesis promoting peptide from Tubulin Alpha-1C chain in Crassostrea gigas, *Food Chemistry*, 2019, **272**, 751-757.
41. J. Lehmann, S. Thiele, U. Baschant, T. D. Rachner, C. Niehrs, L. C. Hofbauer and M. Rauner, Mice lacking DKK1 in T cells exhibit high bone mass and are protected from estrogen-deficiency-induced bone loss, *iScience*, 2021, **24**.
42. V. Domazetovic, Oxidative stress in bone remodeling: role of antioxidants, *Clinical Cases in Mineral and Bone Metabolism*, 2017, **14**, 209-216.
43. V. Ramalingam and R. Rajaram, A paradoxical role of reactive oxygen species in cancer signaling pathway: Physiology and pathology, *Process Biochemistry*, 2021, **100**, 69-81.
44. X.-J. Chen, Y.-S. Shen, M.-C. He, F. Yang, P. Yang, F.-X. Pang, W. He, Y.-m. Cao and Q.-S. Wei, Polydatin promotes the osteogenic differentiation of human bone mesenchymal stem cells by activating the BMP2-Wnt/β-catenin signaling pathway, *Biomedicine & Pharmacotherapy*, 2019, **112**.
45. Y. Liu, M. Ju, Z. Wang, J. Li, C. Shao, T. Fu, Y. Jing, Y. Zhao, Z. Lv and G. Li, The synergistic effect of NELL1 and adipose-derived stem cells on promoting bone formation in osteogenesis imperfecta treatment, *Biomedicine & Pharmacotherapy*, 2020, **128**.
46. W. Pustlauk, T. H. Westhoff, L. Claeys, T. Roch, S. Geißler and N. Babel, Induced osteogenic differentiation of human smooth muscle cells as a model of vascular calcification, *Scientific Reports*, 2020, **10**, 5951.
47. W.-J. Kim, H.-L. Shin, B.-S. Kim, H.-J. Kim and H.-M. Ryoo, RUNX2-modifying enzymes: therapeutic targets for bone diseases, *Experimental & Molecular Medicine*, 2020, **52**, 1178-1184.
48. T. Komori, Regulation of Proliferation, Differentiation and Functions of Osteoblasts by Runx2, *International Journal of Molecular Sciences*, 2019, **20**.
49. M. Ling, P. Huang, S. Islam, D. P. Heruth, X. Li, L. Q. Zhang, D.-Y. Li, Z. Hu and S. Q. Ye, Epigenetic regulation of Runx2 transcription and osteoblast differentiation by nicotinamide phosphoribosyltransferase, *Cell & Bioscience*, 2017, **7**, 27.
50. S. Vimalraj, Alkaline phosphatase: Structure, expression and its function in bone mineralization, *Gene*, 2020, **754**.
51. Q. Liu, M. Li, S. Wang, Z. Xiao, Y. Xiong and G. Wang, Recent Advances of Osterix Transcription Factor in Osteoblast Differentiation and Bone Formation, *Frontiers in Cell and Developmental Biology*, 2020, **8**, 601224.
52. W. Li, Z. Chen, C. Cai, G. Li, X. Wang and Z. Shi, MicroRNA-505 is involved in the regulation of osteogenic differentiation of MC3T3-E1 cells partially by targeting RUNX2, *Journal of Orthopaedic Surgery and Research*, 2020, **15**, 143.
53. Haselamirrah M. Akhir and Peik L. Teoh, Collagen type I promotes osteogenic differentiation of amniotic membrane-derived mesenchymal stromal cells in basal and induction media, *Bioscience Reports*, 2020, **40**, BSR20201325.